

Reducing Biases in Record Matching Through Scores Calibration

Mohammad Hossein Moslemi and Mostafa Milani

Abstract—Record matching is the task of identifying records that refer to the same real-world entity across datasets. While most existing models optimize for accuracy, fairness has become an important concern due to the potential for unequal outcomes across demographic groups. Prior work typically focuses on binary outcomes evaluated at fixed decision thresholds. However, such evaluations can miss biases in matching scores—biases that persist across thresholds and affect downstream tasks.

We propose a threshold-independent framework for measuring and reducing *score bias*, defined as disparities in the distribution of matching scores across groups. We show that several state-of-the-art matching methods exhibit substantial score bias, even when appearing fair under standard threshold-based metrics. To address this, we introduce two post-processing score calibration algorithms. The first, *Calib*, aligns group-wise score distributions using the Wasserstein barycenter, targeting demographic parity. The second, *C-Calib*, conditions on predicted labels to further reduce label-dependent biases, such as equal opportunity.

Both methods are model-agnostic and require no access to model training data. *Calib* also offers theoretical guarantees, ensuring reduced bias with minimal deviation from original scores. Experiments across real-world datasets and matching models confirm that *Calib* and *C-Calib* substantially reduce score bias while minimally impacting model accuracy.

Index Terms—Record Matching, Fairness, Wasserstein Barycenter, Calibration, Threshold Independent.

I. INTRODUCTION

RECORD matching is the task of identifying records from one or more datasets that refer to the same real-world entity. It is important both as a standalone task—such as matching social media profiles across different platforms or identifying duplicate patient health records in healthcare systems—and as a component of broader data processes like data integration and data cleaning.

Record matching is often formulated as a binary classification problem, where pairs of records are labeled as either “match” or “non-match.” However, in practice, most record matching methods output a *matching score* rather than a direct binary label. This score indicates the likelihood of a match: higher values suggest stronger evidence, while lower values imply that the records likely refer to different entities. A binary decision can be derived by applying a threshold to the score.

Having a matching score, rather than only a binary outcome, is important from both application and technical perspectives.

From an application perspective, scores allow adjusting the threshold to balance precision and recall. Lower thresholds

Mohammad Hossein Moslemi and Mostafa Milani (corresponding author) are with the Department of Computer Science, Western University, London, Ontario, Canada (email: mohammad.moslemi@uwo.ca, mostafa.milani@uwo.ca).

increase recall by identifying more matches, but may also increase false positives (FP), leading to incorrect record merges and potential data loss. Higher thresholds reduce FPs but risk missing true matches, which can be critical in domains where missing links between records may result in costly consequences. Matching scores also reflect confidence levels and can be used directly in applications. For example, instead of converting scores to binary decisions, one can use them to rank candidate records and return top matches for a given input. This is useful when showing the most likely matches is more informative than a simple yes-or-no answer.

From a technical perspective, matching scores support the development of more flexible and advanced methods. For example, active learning approaches can use scores to identify uncertain cases—those with values near the decision threshold—and prioritize them for manual labeling to improve the model [1], [2]. This idea also extends to human-in-the-loop systems, where scores help determine which record pairs should be reviewed by a human. Instead of treating all pairs equally, the system can focus on those that are harder to classify automatically [3], [4]. Another technical reason for using scores instead of binary outcome is that many state-of-the-art matching techniques, especially deep learning models, naturally produce scores through their architecture—for example, by applying a sigmoid activation to the output of a final linear layer, resulting in a value between 0 and 1 that reflects the predicted match likelihood. Because of these advantages, matching scores are more widely used than hard binary decisions in both research and practical systems.

In this paper, we study fairness in record matching by focusing on biases in matching scores and propose methods to reduce these biases. Fairness in record matching has received growing attention in recent years, as studies have shown that biases in matching can disproportionately harm minority groups and lead to unfair outcomes [5], [6], [7], [8]. However, prior work has mainly treated record matching as a binary classification task. In contrast, biases in matching scores are more complex and harder to detect and reduce. A score may appear fair under one threshold but produce biased outcomes under another. Moreover, in many applications where scores are used directly—rather than converted to binary decisions—differences in score quality across groups can lead to lower accuracy for minorities and unfair treatment. The following example illustrates how biases in matching scores can be more subtle and problematic than in binary outcomes.

Example 1. Figure 1 shows the performance of HierMatch [9], a state-of-the-art record matching method, on DBLP-ACM—a benchmark of publication records with

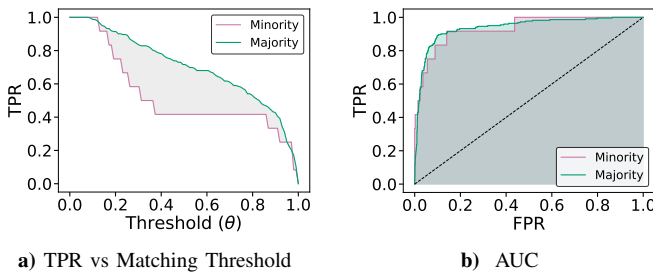


Fig. 1: Figure 1a shows variation in TPR across thresholds. The ROC of HierMatch [9] (Figure 1b) shows that the AUC is nearly the same for both groups, with 93.33% for the minority group and 93.94% for the majority. However, there is a noticeable difference in performance at specific thresholds.

potential duplicates referring to the same paper. We compare the method’s performance on records authored by females as the minority group, versus all other records as the majority group. Figure 1a reports the true positive rate (TPR) for each group and for varying matching thresholds. The gap in TPR near mid-range thresholds reflects bias in binary outcomes. At thresholds near 0 or 1, these gaps disappear, suggesting no bias at those extremes. This demonstrates that score biases depend on the threshold and must be evaluated across the full score range by comparing score distributions across groups.

Figure 1b presents another view of score bias by showing the ROC curves for the two groups. These curves measure the trade-off between TPR and false positive rate (FPR), and their area under the curve (AUC) is often used to assess score quality independent of any specific threshold. Although the ROC curves differ, the AUC values are nearly the same, as the differences cancel out. This shows that aggregate measures like AUC—despite being threshold-independent—can still overlook important biases in score distributions. ■

The most closely related work to fairness in matching scores is the literature on fairness in classification scores for binary classification tasks (e.g., [10], [11], [12]). These approaches primarily rely on AUC-based measures, defining bias as the gap in AUC between majority and minority groups. However, such metrics can be misleading [13], as shown in Example 1. Moreover, our setting differs in that matching scores are often skewed and context-specific, unlike the general case of binary classification. This distinction motivates the need for dedicated techniques to assess and mitigate bias in matching scores.

Fairness in matching scores is also related to fairness in regression [14], [15], [16] and ranking [17], [18], [19], [20], [21], [22]. Like regression, matching scores are continuous, and we adopt a similar strategy of comparing score distributions across groups. However, unlike typical regression outputs, which often span wide or unbounded ranges, matching scores are usually concentrated near 0 and 1. We exploit this property in our bias reduction algorithms.

Fair ranking is also relevant, as both settings involve scoring and ranking inputs. However, fair ranking methods (e.g., [20], [21], [22]) focus on group-level balance among top-ranked items (e.g., top- k). In contrast, fairness in matching scores

aims to ensure equitable outcomes across all score thresholds.

To address fairness in matching scores, our first contribution is a new bias measure that extends standard notions such as demographic parity (DP) and equalized odds (EOD) from binary outcomes to score distributions across all thresholds. It captures cumulative performance differences between groups over the full threshold range. For example, in Figure 1a, the DP score bias is the sum of TPR differences across thresholds, shown by the gray area between the two plots. Using this measure, we evaluate popular benchmarks and state-of-the-art matching methods, revealing substantial score biases.

To reduce these biases, we propose a post-processing algorithm that calibrates scores without altering matching models, making it broadly applicable. The algorithm treats the scores for each demographic group as probability distributions and aligns them by mapping both to a shared target distribution. We use optimal transport (OT) to compute the Wasserstein barycenter [15], [23], which serves as a balanced average that minimizes deviation from the original scores while improving fairness. This approach also offers theoretical guarantees, including an asymptotic upper bound on post-calibration bias that decreases with data size, derived from OT theory.

Empirical results show that our calibration method effectively reduces DP score bias across various benchmarks and matching methods. However, it does not address EOD score bias, which depends on true labels. To tackle this, we introduce *conditional calibration*, a variant that adjusts scores based on both the predicted score and the estimated label. This method significantly reduces EOD score bias, as demonstrated through extensive evaluations on standard benchmarks.

This paper is organized as follows. Section II presents background on record matching, notation, and existing fairness metrics. Section III introduces our proposed fairness metric and formalizes the problem. Sections IV and V describe two bias reduction algorithms. Section VI reports experimental results. Section VII reviews related and Section VIII concludes with a summary and future directions.

II. PRELIMINARIES

A relational schema \mathcal{S} consists of attributes A_1, \dots, A_m , where each attribute A_i has a domain $\text{Dom}(A_i)$ for $i \in [1, m]$. A record (or tuple) r over \mathcal{S} is an element of the Cartesian product $\text{Dom}(A_1) \times \dots \times \text{Dom}(A_m)$, representing the space of all possible records, denoted by \mathcal{R} . The value of attribute A_i in record r is written as $r[A_i]$. A relation (or instance) R over \mathcal{S} is a subset of \mathcal{R} containing a set of records.

A. Record Matching

Given two relations, R_1 and R_2 with schemas \mathcal{S}_1 and \mathcal{S}_2 , *record matching* aims to identify a subset E of record pairs in $R_1 \times R_2$ that refer to the same real-world entities. These are called *equivalent pairs*, while all others are *non-equivalent*. Without loss of generality and for simplicity, we assume $R_1 = R_2$.

A record matcher, or simply a matcher, is a binary classifier $f : \mathcal{R}^2 \rightarrow \{0, 1\}$ that assigns a label of 1 (match) or 0 (non-match) to pairs of records from a relation R with schema \mathcal{S} .

Symbol	Description
R, \mathcal{S}	Relation and schema
r, p	Record and (record) pair
A_1, A_2, \dots	Attributes
A	Binary sensitive (protected) attribute
\mathcal{R}	All possible records
$Dom(A_i)$	Domain of an attribute A_i
$a, b \in Dom(A)$	Minority and majority
$P(X)$	Probability distributions or random variable X
Φ	Performance metric
\tilde{P}	Wasserstein barycenter
s, θ	Matching score function and matching threshold

TABLE I: Summary of notation and symbols.

The goal is to correctly label equivalent pairs as matches and non-equivalent pairs as non-matches.

A matcher f is often defined using a matching score function $s : \mathcal{R}^2 \rightarrow [0, 1]$ and a threshold $\theta \in [0, 1]$. It labels a pair p as a match if $s(p) \geq \theta$, i.e., $f(p) = \mathbb{1}_{s(p) \geq \theta}$.

Performance metrics for f are formally defined with respect to a joint probability distribution P over a random variable X (representing pairs of records from \mathcal{S}) and a binary variable Y indicating the true label. The positive rate (PR), true positive rate (TPR), and false positive rate (FPR) for s and θ are defined as $PR(s, \theta) = P(s(X) \geq \theta)$, $TPR(s, \theta) = P(s(X) \geq \theta \mid Y = 1)$, and $FPR(s, \theta) = P(s(X) \geq \theta \mid Y = 0)$. We use \hat{Y} to refer to $f(X)$ and, when clear from context, write A_i instead of A and $X[A_i]$ for attribute values. Other metrics such as precision, recall, and F1 score are defined similarly. The AUC for s is $\int_0^1 TPR(s, FPR^{-1}(s, \theta)) d\theta$.

B. Fairness Measure in Record Matching

To study fairness in record matching, we assume records contain a sensitive attribute $A \in \mathcal{S}$, such as gender or ethnicity, which defines majority and minority groups. For simplicity, we consider A to be binary, with $Dom(A) = \{a, b\}$, where records with value a belong to the minority group (e.g., female) and those with b to the majority group (e.g., male). A record pair $p = (r_1, r_2)$ is considered a minority pair, denoted by $p[A] = a$, if either record belongs to the minority group, i.e., if $r_1[A] = a$ or $r_2[A] = a$; otherwise, it is a majority pair ($p[A] = b$). This definition ensures that any pair involving a minority record is treated as a minority pair, reflecting that mismatches may disproportionately affect minority records.

1) *Fairness in Binary Matching*: Fairness in record matching, treated as a binary classification task, has been extensively studied in [8]. Several fairness definitions are applied to assess bias, following principles similar to those used in general classification tasks. These definitions examine the relationship between the sensitive attribute $p[A]$ and the matcher's output $f(p)$ for any record pair p . Each definition compares a *performance metric* Φ , such as TPR, FPR, or PR, across sensitive groups, denoted Φ_g for $g \in \{a, b\}$. The corresponding *fairness metric*, or bias, is denoted as $bias(f, \Phi)$.

Demographic parity, or *statistical parity*, requires the positive rate $\Phi = PR$ to be independent of the sensitive attribute, i.e., $\hat{Y} \perp\!\!\!\perp A$. This implies that the probability of matching is the same across groups, regardless of true labels. Formally, $PR_a = PR_b$, where $PR_g = P(\hat{Y} = 1 \mid A = g)$. The associated

fairness metric is the demographic parity difference, given by $bias(f, PR) = |PR_a - PR_b|$.

Demographic parity ignores ground truth equivalence. In contrast, definitions such as *equalized odds* and *equal opportunity* condition on equivalence to evaluate fairness, requiring $\hat{Y} \perp\!\!\!\perp A \mid Y$. *Equal opportunity (EO)*, also known as true positive rate parity, requires $TPR_a = TPR_b$, where $TPR_g = P(\hat{Y} = 1 \mid A = g, Y = 1)$. The corresponding fairness metric is $bias(f, TPR) = |TPR_a - TPR_b|$.

Equalized odds (EOD) extends this further by requiring both TPR and FPR to be equal across groups. A matcher satisfies EOD if $TPR_a = TPR_b$ and $FPR_a = FPR_b$, where $FPR_g = P(\hat{Y} = 1 \mid A = g, Y = 0)$. EOD captures fairness for both positive and negative classes. The fairness metric based on EOD is $bias(f, TPR+FPR) = |TPR_a - TPR_b| + |FPR_a - FPR_b|$.

C. Wasserstein Distance and Barycenter

The *Wasserstein- ρ distance* (W_ρ) quantifies the distance between two probability measures as the minimum cost of transporting mass from one distribution to the other. For univariate distributions P and Q over \mathbb{R} , it is defined as:

$$W_\rho(P, Q) = \left(\inf_{\pi \in \Pi(P, Q)} \int_{\mathbb{R} \times \mathbb{R}} d(x, y)^\rho d\pi(x, y) \right)^{1/\rho} \quad (1)$$

Here, $\Pi(P, Q)$ denotes the set of all *couplings* of P and Q , where each coupling π is a joint distribution over \mathbb{R}^2 with marginals P and Q . A coupling specifies how to assign mass from P to Q while preserving their distributions. Note that the coupling in Eq. 1 is not unique; different couplings can yield different transport costs. The function $d(x, y)$ represents the cost of transporting mass from x to y . For the commonly used W_2^2 , this cost is $d(x, y) = |x - y|^2$ [24].

This formulation follows the *Kantorovich approach* to optimal transport, which allows mass at a source point to be spread probabilistically across multiple target points. This flexibility ensures the existence of an optimal coupling that minimizes total transport cost. In contrast, the *Monge formulation* seeks a deterministic mapping T that transports each source point to a single target point. This is expressed as the *pushforward* $T_\# P = Q$, meaning that applying T to P yields Q . While more intuitive, the Monge approach can be too restrictive or infeasible when the source and target distributions differ significantly in structure.

The *barycenter* of a set of distributions is a representative distribution that balances their characteristics. Depending on the metric used, different types of barycenters can be defined. The *Wasserstein barycenter* minimizes the average Wasserstein distance to a given set of distributions, yielding a central distribution that optimally reflects transport-based similarity. Given k distributions P_1, P_2, \dots, P_k with weights $\alpha_1, \alpha_2, \dots, \alpha_k$, the Wasserstein barycenter \tilde{P} is defined as [25], [26]: $\tilde{P} = \arg \min_P \sum_{i=1}^k \alpha_i W_\rho^2(P, P_i)$. For the special case of two distributions P_1 and P_2 using the Wasserstein-2 distance, this reduces to:

$$\tilde{P} = \arg \min_P \left(\alpha W_2^2(P_1, P) + (1 - \alpha) W_2^2(P_2, P) \right) \quad (2)$$

III. PROBLEM DEFINITION

As discussed in Section II-B, existing fairness definitions are either threshold-specific or, in the case of AUC-based, threshold-independent but potentially misleading. To address these limitations, we introduce a new fairness metric for matching scores, extending binary classification fairness measures (see Section II-B1) to evaluate biases in a score function s across all thresholds.

Definition 1 (Fair matching score). The bias of a matching score function s with respect to a performance metric Φ is defined as

$$\text{bias}(s, \Phi) = \int_0^1 |\Phi_b(s, \theta) - \Phi_a(s, \theta)| d\theta \quad (3)$$

We say s is fair if $\text{bias}(s, \Phi) = 0$.

Definition 1 generalizes fairness notions such as DP, EO, and EOD to score functions. For example, setting $\Phi = \text{PR}$ recovers DP for s , referred to as *score DP*. Similarly, $\Phi = \text{TPR}$ corresponds to score EO, and using both $\Phi = \text{TPR}$ and $\Phi = \text{FPR}$ yields EOD. For any unfair score function, the value of $\text{bias}(s, \Phi)$ quantifies the score bias. For example, $\text{bias}(s, \text{PR})$ measures the DP score bias, $\text{bias}(s, \text{TPR})$ captures the EO score bias, and $\text{bias}(s, \text{TPR}) + \text{bias}(s, \text{FPR})$ represents the EOD score bias. When clear from context, we omit the term “score” and simply refer to these as DP, EO, or EOD biases.

Prior work [8], [5] has shown that many existing record matching methods produce biased matching scores. In Section VI-B1, we demonstrate through experiments on standard benchmarks that several state-of-the-art techniques exhibit substantial bias. To address this, we define the problem of generating fair matching scores and propose a post-processing solution to adjust scores from existing methods.

Definition 2 (FairScore). Given a matching score function s and a performance metric Φ , the FairScore problem seeks an optimal fair score function s^* :

$$s^* = \arg \min_{\text{fair } s'} \text{risk}(s', s) \quad (4)$$

where the risk function is defined as

$$\text{risk}(s^*, s) = \mathbb{E}[|s^*(X) - s(X)|] \quad (5)$$

and X is a random variable over record pairs.

In other words, FairScore aims to find a fair score function that remains close to the original one, minimizing the difference in scores while improving fairness with respect to the chosen performance metric Φ .

IV. SCORE CALIBRATION USING BARYCENTER

This section introduces our first bias reduction algorithm, *Calib* (Algorithm 1), for the FairScore problem with $\Phi = \text{PR}$, where the goal is to remove DP bias. Given a score function s , *Calib* calibrates it into a new function \hat{s} that is independent of group membership. It does so by computing the Wasserstein barycenter of the minority (s_a) and majority (s_b)

score distributions, balancing both groups while minimizing the risk of \hat{s} (Eq. 5).

We first explain the intuition behind the algorithm and then describe the algorithm step by step with an example. We conclude with a discussion of its theoretical properties.

A. Algorithm Description and Analysis

The *Calib* algorithm calibrates scores by estimating the Wasserstein barycenter of the score distributions for each group. It computes the barycenter using *quantile-based barycenter computation* method, a standard approach in optimal transport theory [27] for univariate distributions. In one dimension, the Wasserstein distance becomes a linear transport problem, making this method a natural choice. This method requires absolutely continuous distributions with shared support-conditions typically met by deep learning models that output real-valued scores (e.g., $[0, 1]$). Alternative methods such as Sinkhorn [28] are less effective for univariate cases and are primarily used for multivariate distributions and therefore we did not consider them in our work.

Now, consider the univariate distributions of scores for each group, denoted by P_a and P_b . The algorithm computes the barycenter distribution \tilde{P} of P_a and P_b using the quantile-based method. This approach leverages the *cumulative distribution function (CDF)*, denoted by \mathbb{F} , and its inverse, the *quantile function* (\mathbb{Q}), of each distribution. Specifically, the quantile function for group $g \in \{a, b\}$ is defined as $\mathbb{Q}_g(p) = \mathbb{F}_g^{-1}(p)$, mapping each probability level $p \in [0, 1]$ to its corresponding score in distribution P_g .

The quantile-based method calculates the barycenter quantile function, $\tilde{\mathbb{Q}}(p)$, as a weighted average of the quantile functions of the original distributions:

$$\tilde{\mathbb{Q}}(p) = \alpha \mathbb{Q}_a(p) + (1 - \alpha) \mathbb{Q}_b(p),$$

where $\alpha = P(A = a)$ and $1 - \alpha = P(A = b)$. These weights represent the relative contributions of each group distribution to the barycenter. The resulting barycenter distribution \tilde{P} integrates characteristics from both original distributions. Finally, the algorithm returns the calibrated score $\hat{s}(p)$ derived from the barycenter distribution. Algorithm 1 summarizes this process.

Before detailing each step in Algorithm 1, we clarify a few key points. First, in practice, the distributions P_a and P_b are unknown, which prevents direct use of the quantile method. Instead, the algorithm uses score functions s_a and s_b , generating i.i.d. samples of scores from randomly selected pairs. To improve robustness, Gaussian noise (commonly known as jitter) is added to these samples (Line 5 in Algorithm 1) [29]. Jitter helps reduce ties in the scores, ensuring continuity and smoother quantile transitions. To estimate the CDFs of P_a and P_b , the algorithm employs the *plug-in method* based on observed data D [30], [31]. Specifically, it uses sorted score samples (scores_a and scores_b) along with the position parameter pos to empirically estimate quantile values. Although alternatives such as kernel density estimation or parametric fitting exist, the plug-in method is favored here for its simplicity, robustness, and consistency, facilitating effective computation of the barycenter’s quantile function.

Algorithm 1: $\text{Calib}(D, s, p)$

Input: A set of record pairs $D = \{p_1, \dots, p_{|D|}\}$; a matching score function s , a query pair p
Output: Calibrated score for p

```

1  /* Initialize group score lists */
2  scoresb ← []; scoresa ← [];
3  foreach  $p_i \in D$  do
4     $g \leftarrow p_i[A]$ ;      /* Identify pair group */
5    append(scoresg,  $s(p_i) + \mathcal{N}(0, \sigma^2)$ );
6  sort(scoresa); sort(scoresb);
7   $g \leftarrow p[A]$ ;          /* Identify query pair group */
8  posg ← 0;               /* Initialize insertion point */
9  while posg < |scoresg| and scoresg[posg] > s(p) do
10   posg ← posg + 1;
11   $\alpha \leftarrow \frac{|scores_a|}{|D|}$ ;  $q \leftarrow \frac{pos_g}{|scores_g|}$ ; /* Compute quantile */
12  posḡ ← ⌈ q × |scoresḡ| ⌉; /* Cross-group map */
13  return  $\alpha \times scores_a[pos_a] + (1 - \alpha) \times scores_b[pos_b]$ ;

```

The second point concerns the input dataset $D = \{p_1, \dots, p_{|D|}\}$, used to estimate P_a and P_b . This dataset does not require ground-truth labels—only matching scores are needed, which can be obtained by applying the score function s . As a result, s can be calibrated as a black box without access to the training data used to learn s , such as in deep learning-based matchers. This significantly broadens the applicability of the calibration method. The only assumption is that the pairs in D are i.i.d. samples from the space of possible record pairs and that the dataset is large enough to reliably estimate the score distributions. The primary goal of the algorithm is to calibrate the scores for one or more query pairs. When the number of query pairs is large enough (as discussed in Section IV-B), the dataset D can simply be the set of query points itself. We examine the effect of choosing a dataset D with a distribution different from that of the query points in Section VI-B5. We now describe each step of Algorithm 1.

Algorithm 1 takes the dataset D , a biased score function s (i.e., $\text{bias}(s, \text{PR}) > 0$) and a query pair p , and returns a calibrated score $\hat{s}(p)$. This calibrated score approximates the optimal fair score s^* , which solves FairScore for the fairness metric $\Phi = \text{PR}$, removing DP bias. The algorithm begins by initializing two empty lists to store scores separately for minority and majority groups (Line 2). For each record pair in the dataset D , it identifies the group based on the sensitive attribute (Line 4) and appends the computed score from s , with added Gaussian noise for smoothing, to the appropriate group's list (Line 5). This noise also ensures that $s(p_i) + \mathcal{N}(0, \sigma^2)$ forms i.i.d. and continuous samples of $s(X)$, a property we later use in Theorem 1. After processing all record pairs, the score lists for both groups are sorted in descending order (Line 6). Note that as long as the observed dataset D remains unchanged, these parts of the algorithm need to be executed only once for more than one query pair.

To calibrate the score for a query pair p , the algorithm identifies the group g of p (Line 7) and initializes a pos variable within the sorted score list (Line 8). It then iterates through the sorted scores to locate the position where $s(p)$

would fit, counting scores greater than $s(p)$ within group g (Lines 9–10). This position, relative to the list length, defines a quantile q , representing the percentage of scores in group g greater than $s(p)$ (Line 11). The algorithm then calculates $\text{pos}_{\bar{g}} = \lceil q \times |scores_{\bar{g}}| \rceil$, where \bar{g} is the opposite group (i.e., if $g = a$, then $\bar{g} = b$, and vice versa). This position is used to find the score in the other group's list that corresponds to the same quantile q as the query score in its own group.

Finally, the algorithm returns the calibrated score as a weighted average of the scores at the identified positions in both groups' sorted lists. The returned calibrated score is $\alpha \times scores_a[pos_a] + (1 - \alpha) \times scores_b[pos_b]$ (Line 13). Here, α is the proportion of minority group scores in D (Line 12). Now, we provide an example to illustrate the algorithm's steps.

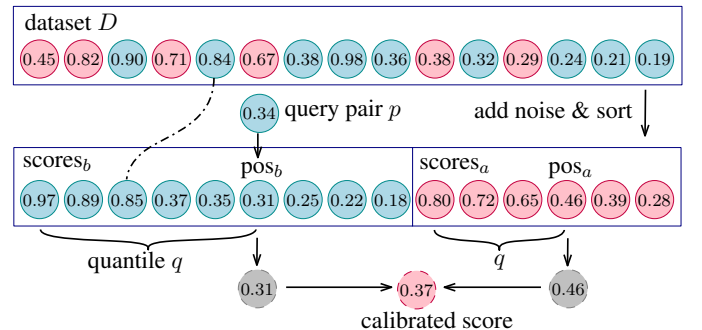


Fig. 2: Running Algorithm 1 in Example 2

Example 2. Consider dataset D shown in Figure 2, containing 15 record pairs scored by s and labeled a or b by a sensitive attribute. The pairs and scores are: (0.45, a), (0.82, a), (0.90, b), (0.71, a), (0.84, b), (0.67, a), (0.38, b), (0.98, b), (0.36, b), (0.38, a), (0.32, b), (0.29, a), (0.24, b), (0.21, b), (0.19, b). Following the calibration algorithm, Gaussian noise $\mathcal{N}(0, 0.05^2)$ is added to each score, resulting in the following (rounded) values: (0.46, a), (0.80, a), (0.89, b), (0.72, a), (0.85, b), (0.65, a), (0.37, b), (0.97, b), (0.35, b), (0.39, a), (0.31, b), (0.28, a), (0.25, b), (0.22, b), (0.18, b). Sorting these in descending order gives scores_b = [0.97, 0.89, 0.85, 0.37, 0.35, 0.31, 0.25, 0.22, 0.18] and scores_a = [0.80, 0.72, 0.65, 0.46, 0.39, 0.28]. Suppose the query pair p has a score $s(p) = 0.34$ and belongs to the b group. The algorithm sets $g = b$ and $pos = 0$. It then performs a linear search to find the position of 0.34 within scores_b, which falls between 0.31 and 0.35, so $pos_b = 6$. Next, α is calculated as the proportion of minority scores, $\alpha = |scores_a|/|D| = 6/15 = 0.4$, and the quantile $q = pos_g/|scores_g| = 6/9 \approx 0.67$. Using q , we compute the corresponding position in the minority scores: $pos_a = \lceil q \times |scores_{\bar{g}}| \rceil = 0.67 \times 6 \approx 4$, giving the score 0.46 in the minority group. Finally, we compute a weighted average of the scores 0.31 and 0.46 using weights α and $1 - \alpha$, resulting in the calibrated score $\hat{s}(p) = 0.4 \times 0.46 + 0.6 \times 0.31 = 0.37$. Thus, the algorithm returns a calibrated score of 0.37 for the query pair p . The steps are illustrated in Figure 2. ■

B. Theoretical guarantees

Algorithm 1 returns a calibrated score for any given query pair, and therefore, in essence, it computes a score function \hat{s} . In the following theorem, s is the input score function, \hat{s} is the calibrated score function, and s^* is the optimal matching score function (Definition 2). Let n_a and n_b denote the number of the minority and majority samples in D . The theorem provides an upper bound on the bias of \hat{s} and asymptotically upper bounds its risk, limiting \hat{s} deviation from s^* .

Theorem 1. *For the calibrated score \hat{s} obtained from Algorithm 1, with input score s and optimal score function s^* , the following asymptotic bounds hold, where $n = \min(n_a, n_b)$:*

$$\text{bias}(\hat{s}, \text{PR}) = O(n^{-1}), \quad (6)$$

$$\text{risk}(s^*, \hat{s}) = O(\log(n)^{-1/2}). \quad (7)$$

Proof. To prove Eq. 6, we start from the left-hand side:

$$\begin{aligned} \text{bias}(\hat{s}, \text{PR}) &= \int_0^1 |\text{PR}_a(\hat{s}, \theta) - \text{PR}_b(\hat{s}, \theta)| d\theta \\ &= \int_0^1 |P_a(\hat{S} \geq \theta) - P_b(\hat{S} \geq \theta)| d\theta \\ &= \int_0^1 |(1 - P_a(\hat{S} \leq \theta)) - (1 - P_b(\hat{S} \leq \theta))| d\theta \\ &= \int_0^1 |P_a(\hat{S} \leq \theta) - P_b(\hat{S} \leq \theta)| d\theta. \end{aligned} \quad (8)$$

Here, $P_g(\hat{S}) = P(\hat{s}(X) = \hat{S}|A = g), g \in \{a, b\}$ and P is the barycenter of P_a^s and P_b^s . The integral of a function over $[0, 1]$ is always bounded by the function's supremum on $[0, 1]$. Thus, from Eq. 8, we deduce:

$$\text{bias}(\hat{s}, \text{PR}) \leq \sup_{\theta \in [0, 1]} |P_a(\hat{S} \leq \theta) - P_b(\hat{S} \leq \theta)| \quad (9)$$

Since P is a barycenter obtained from the quantile-based method; we write the right-hand side of Eq. 9 as follows:

$$\text{bias}(\hat{s}, \text{PR}) \leq \sup_{\theta \in [0, 1]} |P(\mathbb{F}_a(s(X)) \leq \theta) - P(\mathbb{F}_b(s(X)) \leq \theta)| \quad (10)$$

where \mathbb{F}_g is the CDF of the scores for group g . This means an estimation of $P(\mathbb{F}_g(s(X)) \leq \theta)$ is $m_g/(n_g + 1)$ where $m_g, g \in \{a, b\}$ is the number of pairs p in D that are from group g and $s(p) < \theta$. Therefore, we write Eq. 10 as

$$\text{bias}(\hat{s}, \text{PR}) \leq \sup_{\theta \in [0, 1]} \left| \frac{m_a}{n_a + 1} - \frac{m_b}{n_b + 1} \right| \quad (11)$$

Since $0 \leq m_g \leq n_g$, the difference is maximized when one group has $m_g = 0$ and the other $m_{\bar{g}} = n_g$, yielding a worst-case difference rate of $O(1/\min(n_a, n_b)) = O(n^{-1})$.

The proof of Eq. 7 relies on the fact that the score \hat{s} , obtained from the average barycenter of s_a and s_b , has the minimal risk. The barycenter minimizes risk by reducing the total Wasserstein distance. Since risk is defined as the expected difference between the calibrated score and the original score, it is directly tied to the transport cost in the Wasserstein distance. The barycenter ensures that adjustments to align group-specific score distributions are as small as possible. The

cost function $|x - y|^2$ in the Wasserstein distance quantifies the effort required to modify scores, which directly affects the expected deviation. By minimizing this cumulative transport cost, the barycenter produces a calibrated score that reduces bias while making minimal changes to the original scores. This property makes it a theoretically optimal solution for balancing fairness and accuracy in score calibration.

The proof uses the following concentration inequality, commonly applied in statistical learning theory [32], [33]:

$$P(|\tilde{s}(X) - \hat{s}(X)| \geq \delta) \leq c \exp(-Cb_n \delta^2), \quad (12)$$

where c and C are constants, b_n depends on the sample size, and $\exp(-Cb_n \delta^2)$ reflects the rapid decay of probability as δ grows. Integrating this inequality over all possible deviations bounds the risk:

$$E[|\tilde{s}(X) - \hat{s}(X)|] = \int_0^\infty P(|\tilde{s}(X) - \hat{s}(X)| \geq \delta) d\delta. \quad (13)$$

Substituting the tail probability and solving the integral gives:

$$E[|\tilde{s}(X) - \hat{s}(X)|] \leq \frac{c\sqrt{\pi}}{2\sqrt{Cb_n}} = O(b_n^{-1/2}). \quad (14)$$

For deep learning models used in classification, including those applied to matching in this work, the rate parameter b_n is typically $\log(n)$ due to the high capacity of neural networks and implicit regularization effects [34], [35], [36]. Substituting $b_n = \log(n)$ yields the upper bound $O(\log(n)^{-1/2})$. ■

Theorem 1 shows that as the sample size increases, the bias of \hat{s} vanishes and its risk reaches the minimum value. As a result, the calibrated score function \hat{s} converges to the optimal score function s^* , achieving both fairness and accuracy. Also, this theorem specifies what “sufficiently large” dataset D means in Section IV-A. From Eq. 6, if the maximum allowable bias after calibration is ϵ , then the dataset must satisfy $|D| \geq O(\frac{1}{\epsilon})$.

V. CONDITIONAL CALIBRATION

Although the Calib algorithm ensures DP, it does not satisfy other fairness criteria, such as EOD and EO, because these definitions rely on the true (matching) labels of pairs- a factor not considered by Calib. To address this, we introduce *conditional calibration* (C-Calib), as shown in Algorithm 2. C-Calib estimates the unknown true labels, enabling it to meet fairness definitions that depend on label information. Like the original calibration algorithm, C-Calib reduces the correlation between \hat{Y} and A , but it conditions this adjustment on Y , enforcing $\hat{Y} \perp\!\!\!\perp A \mid Y$. This produces a fair score distribution that meets fairness criteria such as EO and EOD.

The core idea behind Algorithm 2, is to include predicted labels using variables *matched* and *matched_i*. Here, *matched* is the predicted label for the query pair p , while *matched_i* is the predicted label for each pair in D . This is illustrated in Lines 4 and 8 of Algorithm 2. To estimate labels- whether for the query pair or pairs in D - we require a decision threshold to assign predicted labels based on scores. In traditional binary classification, this threshold is determined on a labeled validation set to optimize a performance metric

Algorithm 2: C-Calib(D, s, p)

Input: $D = \{p_1, \dots, p_{|D|}\}$, s , and a query pair p
Output: Calibrated score for p

- 1 $\text{scores}_b \leftarrow []$; $\text{scores}_a \leftarrow []$;
- 2 */* Find optimal decision threshold */*
- 3 $\gamma \leftarrow \text{meanshift}(D)$;
- 4 $\text{match} \leftarrow \mathbb{1}(s(p) \geq \gamma)$; */* Label query pair */*
- 5 $\text{size} \leftarrow 0$; */* Size of matched pairs set */*
- 6 **foreach** $p_i \in D$ **do**
- 7 $g \leftarrow p_i[A]$;
- 8 $\text{match}_i \leftarrow \mathbb{1}(s(p_i) \geq \gamma)$; */* Labels pairs */*
- 9 **if** $\text{match} = \text{match}_i$ **then**
- 10 append($\text{scores}_g, s(p_i) + \mathcal{N}(0, \sigma^2)$);
- 11 $\text{size} \leftarrow \text{size} + 1$;
- 12 **sort**(scores_a); **sort**(scores_b); $g \leftarrow p[A]$; $\text{pos}_g \leftarrow 0$;
- 13 **while** $\text{pos}_g < |\text{scores}_g|$ **and** $\text{scores}_g[\text{pos}_g] > s(p)$ **do**
- 14 $\text{pos}_g \leftarrow \text{pos}_g + 1$;
- 15 $\alpha \leftarrow \frac{|\text{scores}_a|}{\text{size}}$; $q \leftarrow \frac{\text{pos}_g}{|\text{scores}_g|}$;
- 16 $\text{pos}_{\bar{g}} \leftarrow \lceil q \times |\text{scores}_{\bar{g}}| \rceil$;
- 17 **return** $\alpha \times \text{scores}_a[\text{pos}_a] + (1 - \alpha) \times \text{scores}_b[\text{pos}_b]$;

(e.g., F1-score) and then applied to unlabeled test data. In our case, we only have a query pair and a set D of observed pairs. To choose an effective decision threshold, we use a non-parametric clustering algorithm, *meanshift* [37], as shown in Line 3. The meanshift algorithm places a window around each data point, computes the mean within the window, and shifts the window toward the mean until convergence. This process clusters points around the modes of the distribution. When applied to score values, which tend to cluster near 0 and 1 (which is the case for record matching problem), the algorithm identifies two clusters. The decision threshold, denoted as γ , is then set as the midpoint between the centers of these clusters, effectively separating the data into two classes without the need for labeled data.

The parameter γ has two purposes in C-Calib. In Line 4, it estimates the label of query pair, and in Line 8, it separates the samples in D into positive and negative samples, assuming D is unlabeled. Unlike decision threshold of θ in the final down-stream applications, γ is specific to the calibration algorithm and does not decide the final label of p . While γ might appear inconsistent with a threshold-agnostic algorithm, it acts as a tuning parameter rather than a classification threshold. By “threshold-agnostic,” we mean the algorithm mitigates bias across all classification thresholds in the final results.

Moving forward, using the conditional check in Line 9, the algorithm adjusts scores based on the query pair’s predicted label. If the query pair is predicted as positive, only pairs in D predicted as positive are included in the calibration; the same applies for a negative prediction. The remainder of the algorithm follows the process of Algorithm 1 described in Section IV-A. We call this approach “conditional” because it calibrates only among pairs sharing the same predicted label as the query pair, consequently enforcing EOD and EO. Now, we demonstrate the entire process with the following example.

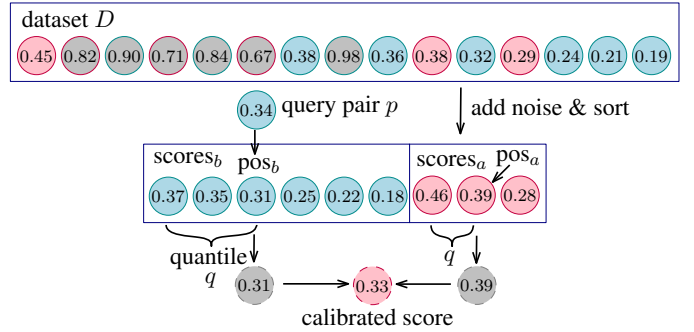


Fig. 3: Running Algorithm 2 in Example 3

Example 3. Following Example 2, consider a dataset D containing 15 pairs with scores as shown in Figure 3. Using meanshift, the decision threshold is set to $\gamma = 0.57$, and the query pair p is predicted as 0 (nonmatch). As a result, the calibration process is applied only to pairs predicted as nonmatches (label 0). As shown in Figure 3, the matched pairs are filtered out, and the remaining pairs are calibrated as in Algorithm 1. This leads to sorted scores in descending order $\text{scores}_b = [0.37, 0.35, 0.31, 0.25, 0.22, 0.18]$ and $\text{scores}_a = [0.46, 0.39, 0.28]$. Next, we calculate $\text{size} = 9$ (the total number of non-matching pairs in D to be used instead of $|D|$ for computing α), with $|\text{scores}_a| = 3$ and $|\text{scores}_b| = 6$. The positions are $\text{pos}_a = 2$ and $\text{pos}_b = 3$ with quantile $q = 0.5$. We also compute $\alpha = |\text{scores}_a|/\text{size} = 3/9 = 0.33$. The calibrated score is calculated as $\hat{s}(p) = 0.33 \times 0.39 + 0.67 \times 0.31 \approx 0.33$. Therefore, the CondCalibrate algorithm returns a calibrated score of 0.33 for the query pair p . ■

Proving the convergence of the calibrated score function \hat{s} from C-Calib is challenging and depends on the quality of the initial score function, as it affects the estimation of labels for D and the query pair p . Empirically, we show that the algorithm effectively reduces bias while maintaining low risk.

VI. EXPERIMENTS

In our experiments, we first assess bias in existing matching methods using our score bias metric. Second, we show that this metric captures bias in matching tasks more effectively than traditional binary measures (Section VI-B1). Third, we evaluate our calibration algorithms for their ability to reduce score bias while maintaining low risk. Bias reduction results are presented in Sections VI-B2 and VI-B3, with risk analysis in Section VI-B4. Finally, we examine the impact of different input dataset D selections in Section VI-B5.

A. Experimental Setup

Before presenting our results, we describe the experimental setup, including datasets and matching methods. All implementations and findings are available in our repository [38].

1) *Datasets:* We used record matching benchmarks [39]: Beer (BEER), Walmart-Amazon (WAL-AMZ), Amazon-Google (AMZ-GOO), Fodors-Zagat (FOD-ZAG), iTunes-Amazon (ITU-AMZ), DBLP-GoogleScholar (DBLP-GOO), and DBLP-ACM (DBLP-ACM). Table II summarizes each

dataset statistics. None of these datasets explicitly denotes a sensitive attribute, we follow prior work [7], [8], [40] to define minority and majority based on the following criteria:

- **DBLP-ACM**: the “authors” attribute contains a female name.
- **FOD-ZAG**: the “Type” attribute equal to “Asian.”
- **AMZ-GOO**: with “Microsoft” as the “manufacturer.”
- **WAL-AMZ**: the “category” attribute equal to “printers.”
- **DBLP-GOO**: “venue” containing “vlldb j.”
- **BEER**: “Beer Name” contains “red.”
- **ITU-AMZ**: the “Genre” attribute containing “Dance.”

Dataset	#Attr.	Dataset Size		Eq%		Sens. Attr.
		Train	Test	Train	Test	
WAL-AMZ	5	8,193	2,049	9.39	9.42	Category
BEER	4	359	91	15.04	15.38	Beer Name
AMZ-GOO	3	9,167	2,293	10.18	10.21	Manufacturer
FOD-ZAG	6	757	190	11.62	11.58	Type
ITU-AMZ	8	430	109	24.42	24.77	Genre
DBLP-GOO	4	22,965	5,742	18.62	18.63	Venue
DBLP-ACM	4	9,890	2,473	17.96	17.95	Authors

TABLE II: Datasets and their characteristics. *Dataset Size* shows training and test set sizes. *Eq%* columns represent the percentage of equivalence pairs in the training and test data.

2) *Record Matching Methods*: We selected five high-performing deep learning record-matching methods with diverse architectures to demonstrate our calibration method’s versatility. DeepMatch combines tokenized inputs, pre-trained embeddings, and metadata, achieving strong performance on structured data [39]. HierGAT employs a Hierarchical Graph Attention Transformer for contextual embeddings [41]. DITTO enhances pre-trained language models with text summarization, data augmentation, and domain expertise [42]. EMTransform uses transformers to model relationships across attributes [43]. HierMatch builds on DeepMatch with cross-attribute token alignment and attribute-aware attention [9]. EMTransform is based on pre-trained transformers and language models [43]. Each model is trained for 100 epochs, with early stopping if the F1 score fails to improve for 15 epochs. The data is split 75% for training and 25% for validation. After training, the model generates scores for the test set, which feed into our calibration algorithms.

B. Experimental Results

We now present our results. For simplicity, we denote matching score biases s as DP, EO, and EOD, corresponding to $bias(s, PR)$, $bias(s, TPR)$, and $bias(s, TPR) + bias(s, FPR)$, respectively. We also use DP_θ and EOD_θ to represent the demographic disparity and equalized odds difference for a matcher with score function s and threshold θ (e.g., $DP_{0.5}$ for $\theta = 0.5$ indicates the conventional demographic disparity).

1) *Biases in Matching Scores*: Here, we analyze the matching methods and their associated biases. Table III summarizes these biases across datasets and matching models. Each metric is reported for three different thresholds, alongside the bias metric for score values as defined in this work. Due to space limitations, we present a subset of model-dataset combinations here; the complete results are available in our repository [38].

An initial look at the table shows that traditional fairness metrics can vary significantly across thresholds. For example, the biases highlighted in blue indicate a notable disparity with $EO_{0.1} = 14$, but much lower biases for $EO_{0.5} = 1.35$ and $EO_{0.95} = 3.38$. Similarly, the biases highlighted in green show minimal bias for $DP_{0.1} = 0.05$ but much higher biases for $DP_{0.5} = 4.85$ and $DP_{0.95} = 3.49$. Similar trends are evident for EOD across methods and datasets. The score bias metrics shown with DP, EO, and EOD provide an aggregate view of biases across all thresholds, capturing overall bias effectively. The results in the table also reveal differences in biases across methods and datasets. In most cases, substantial biases are present, indicating a clear need for debiasing methods.

Dataset	DP	DP $_\theta$			EO	EO $_\theta$			EOD	EOD $_\theta$			
		0.1	0.5	0.95		0.1	0.5	0.95		0.1	0.5	0.95	
DeepMatch	FOD-ZAG	2.86	5.0	2.45	1.92	5.5	0	5.3	15.8	5.8	2.19	5.3	15.8
	DBLP-GOO	6.2	6.6	6.6	1.80	11.5	7.6	10.8	7.9	11.8	7.8	11.0	8.0
	AMZ-GOO	8.9	13.5	9.6	2.30	4.40	14.0	1.35	3.38	8.2	20.7	5.3	3.86
	DBLP-ACM	3.60	4.50	3.90	0.82	1.55	1.05	1.57	7.8	1.80	1.51	1.70	7.8
HierGAT	FOD-ZAG	2.33	2.45	2.45	1.17	7.1	5.3	5.3	15.8	7.1	5.3	5.3	15.8
	DBLP-GOO	5.3	5.3	5.4	5.0	3.40	3.83	2.85	3.95	3.90	4.60	3.22	4.60
	AMZ-GOO	11.1	14.8	11.7	4.14	15.0	11.3	13.5	14.9	19.5	18.3	18.2	15.8
	DBLP-ACM	4.40	4.70	4.30	4.09	0.44	0.80	0.27	0.01	0.66	1.20	0.30	0.22
HierMatch	FOD-ZAG	2.93	1.34	3.09	3.09	0.50	0	0	0	1.41	0.71	0	0
	DBLP-GOO	5.4	7.9	5.8	3.83	4.40	1.15	5.6	8.9	5.3	6.3	5.8	8.9
	AMZ-GOO	9.1	1.84	10.7	4.28	22.0	1.80	33.8	8.8	26.3	5.1	38.1	9.9
	DBLP-ACM	3.89	0.05	4.85	3.49	1.04	0	0.79	0.64	1.70	0.06	1.61	0.76

TABLE III: We evaluated the distributional disparity across models and datasets. Our metrics were compared against traditional fairness measures at thresholds of 0.1, 0.5 and 0.95.

To further demonstrate the importance of biases for scores (Distributional DP or EO), we analyze two examples from Table III in more detail. These examples are highlighted in Table III and shown in Figure 4. Figure 4a illustrates DP_θ across varying thresholds for HierMatch on DBLP-ACM, while Figure 4b shows EO_θ for DeepMatch on AMZ-GOO. As seen in these figures, a model may appear fair at certain thresholds (with narrow color shade widths) based on traditional fairness metrics. However, at thresholds very close to these fair points, the model often displays significant bias toward one group, complicating fairness evaluation. In both figures, the entire colored area effectively represents the distributional disparity.

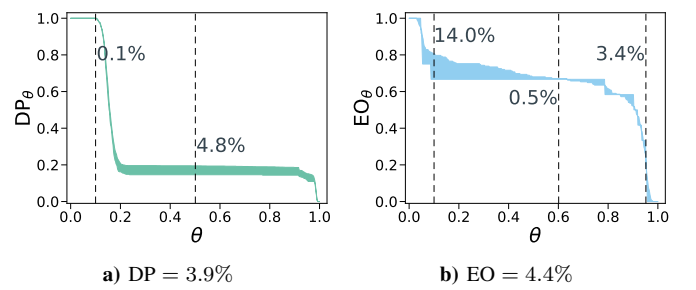


Fig. 4: Variation of bias across thresholds, highlighting the limits of single-threshold fairness assessments. Figure 4a shows this for DBLP-ACM dataset with HierMatch, while Figure 4b does for AMZ-GOO dataset with DeepMatch.

2) *Bias Reduction through Calibration*: Here, we analyze the performance of Calib. For input dataset D , we used the entire test dataset and update query points within this dataset. Figure 5 presents selected results, showing a notable reduction in score bias DP before and after calibration across models and datasets. This shows the effectiveness of the algorithm in minimizing DP and, in many cases, nearly eliminating bias. Due to space limitations, we display a subset of results; similar findings for other combinations are available in our repository. Overall, this calibration approach effectively reduces DP across all tested algorithms and datasets.

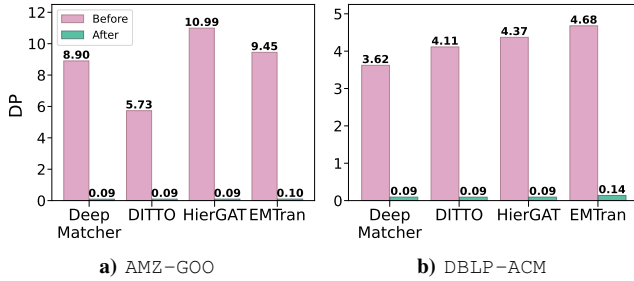


Fig. 5: Comparison of distributional demographic disparity across different models and datasets before and after Calib.

3) *Bias Reduction in Conditional Calibration*: In this section, we first show that Calib is not suitable for addressing biases beyond DP. This is because reducing DP only requires similar score distributions between subgroups, which is insufficient to satisfy fairness criteria such as EO. To overcome this, we use our alternative solution, C-Calib. In this section, we again use the entire test dataset as the input dataset D .

Figure 6 compares the effectiveness of Calib and C-Calib in reducing EO and EOD. As shown, Calib only reduces EO and EOD in a few cases (e.g., HierGAT on BEER); in most instances, it fails to reduce these biases because it does not incorporate label information. This figure demonstrates that Calib's effect on EO and EOD is inconsistent: in some cases, it reduces bias, while in others it increases bias or has no impact. This variability arises from differences in label distributions and the matching quality of methods.

Figure 6 also shows the results for C-Calib. As evident in this Figure, there is a notable improvement in reducing both EO and EOD across all models and datasets compared to Calib. The conditional approach is more effective in reducing these fairness metrics, which aligns with its design of adjusting score distributions conditioned on estimated labels. For instance, C-Calib in AMZ-GOO dataset (Figure 6a), reduced EOD more effectively across all models compared to Calib. Specifically, HierGAT's EOD for AMZ-GOO was increased to 30.92% from its initial value of 19.50% by Calib, however C-Calib reduced it to 7.39%. Similarly, in BEER dataset (Figure 6b), the EO for DITTO on HierGAT are significantly reduced to near-zero values post C-Calib, indicating a strong improvement from Calib. Notably, for DITTO on BEER dataset in Figure 6b, the initial EO was 0.30%, which is already minimal, but the C-Calib further reduced it to 0.13%, highlighting the effectiveness of this

method. Across other datasets (available in our repository), this pattern of reduced disparity by C-Calib continues, showing that the conditional approach better aligns score distributions across demographic groups by estimating labels.

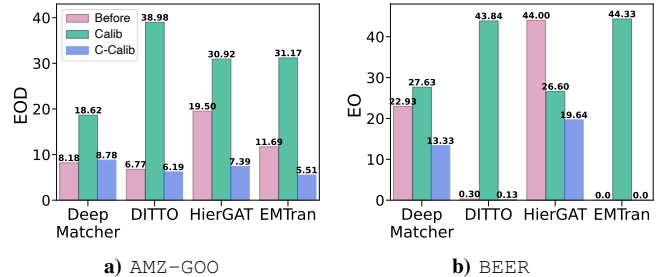


Fig. 6: Comparison of EO and EOD across different models and datasets before and after Calib and C-Calib.

To analyze why Calib fails to reduce certain biases, we present Figure 7. This figure illustrates HierGAT on AMZ-GOO dataset, showing EO and EOD across thresholds before and after calibration. In each plot, the width at each threshold shows the bias magnitude at that threshold. Figures 7a and 7b show that after applying Calib, EO increases from 14.97% to 26.15% and EOD from 19.50% to 30.92%. This highlights Calib's limitation in addressing these metrics, as it does not consider labels. Additionally, before calibration, minority group exhibits lower values compared to majority group (visible as a more discrete edge in the plot due to the minority's smaller sample size). Post-calibration, values for majority group drop while those for minority group increase. This suggests that aligning score distributions with targeted adjustments for minority group might help address EO and EOD, however it would require changes beyond Calib.

Similarly, Figures 7c and 7d shows the effect of C-Calib in the same setting. By comparing this figures with the performance of Calib on this model and dataset, it is clear that C-Calib performs substantially better at reducing EO and EOD biases. Here, C-Calib reduces EO bias from 14.97% to 6.24% and EOD from 19.50% to 7.39%. This reduction shows the effectiveness of C-Calib in aligning score distributions conditioned on estimated labels and achieving improved fairness across thresholds. It is also evident that EO and EOD biases are reduced almost consistently across all thresholds.

Furthermore, by examining the edge for the minority group (a more step-like edge) in Figure 7c and Figure 7d, we observe that the degree of change in scores for both groups is controlled, causing the two edges to move closer together without crossing each other. This results in a reduction in bias. As a result, this algorithm effectively controls the magnitude of score adjustments, which helps mitigate bias.

The main takeaway here is that Calib is highly effective in reducing DP but is not suitable for reducing EO and EOD biases. In contrast, C-Calib provides a more effective bias reduction approach for EO and EOD compared to Calib.

4) *Risk of Calibration*: To conclude our analysis, we examine the impact of Calib and C-Calib on the risk. Risk, as defined in Definition 2, refers to the deviation of

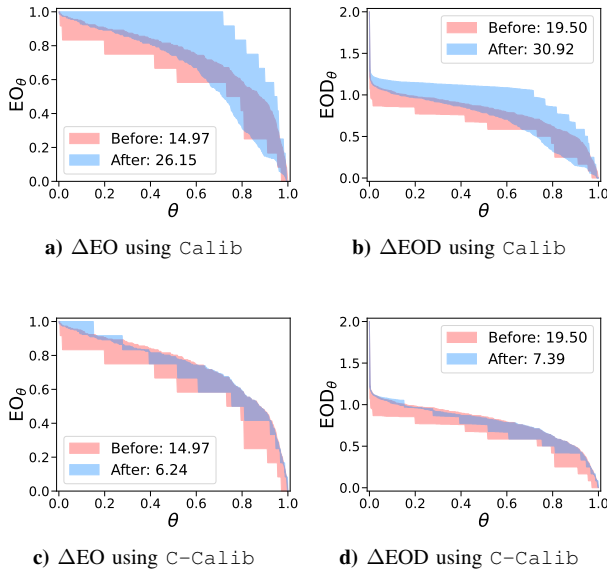


Fig. 7: Comparison of EO and EOD differences, before and after calibration across various thresholds for HierGAT on AMZ-GOO dataset using Calib and C-Calib.

calibrated scores from the initial scores. We evaluate this by comparing the accuracy of the matching scores before and after calibration using the AUC metric. Any decrease in AUC indicates a departure from the initial scores that provided a higher AUC. The focus on AUC, rather than other metrics such as F1-Score or precision, is intentional, as these metrics are threshold-dependent. This choice aligns with the goal of this work to provide a threshold-independent analysis.

Table IV shows the effect of Calib and C-Calib on AUC for AMZ-GOO and DBLP-GOO datasets across matching models. For clarity, only the AUC decreases after calibration are reported. In all cases, both algorithms have minimal AUC reductions, and similar results are observed universally, however only a subset of results is reported due to space constraints. In AMZ-GOO dataset, AUC decrease post-calibration using Calib at most 1.01%. Note that a maximum reduction of 1.01% in AUC results in almost completely removing DP bias from an initially significant value. Similarly, in DBLP-GOO dataset, there is almost no change in AUC after calibration using Calib across different matchers, indicating that Calib effectively reduces DP without compromising accuracy.

Another important observation in this table is that C-Calib achieves slightly better stability in AUC compared with Calib. For instance, in AMZ-GOO, DITTO’s AUC decreases only 0.28%, a minor difference compared to the larger drop of 1.01% for Calib. This trend is similar across other models and datasets, and sometimes, the AUC shows almost no change for C-Calib. This improvement suggests that C-Calib better preserves model performance, which can be attributed to its consideration estimated labels during calibration.

Overall, these results show that both Calib and C-Calib achieves their fairness objective, reducing bias while minimizing risk, and even when the initial bias is significant, the reduction in AUC does not exceed 1%, which is impressive.

Model	AMZ-GOO			DBLP-GOO		
	Before	Calib	C-Calib	Before	Calib	C-Calib
DITTO	96.72	-1.01	-0.28	99.70	-0.11	-0.01
HierGAT	96.93	-0.99	-0.11	99.72	-0.10	-0.01
EMTransform	96.15	-0.97	-0.24	98.72	-0.05	-0.01
HierMatch	90.06	-1.01	-0.06	99.34	-0.10	0.0

TABLE IV: Comparison of AUC. *Before* is the baseline AUC prior to calibration. Calib and C-Calib columns show changes in AUC after each calibration algorithm.

5) *Role of Input Dataset D*: In this section, we evaluate the effect of selecting different input datasets D for the Calib algorithm. Similar trends were observed for the C-Calib algorithm. Table V shows the results of applying two matching models on four benchmark datasets, comparing two calibration settings: first using the same set of query points as the input dataset D , and second using a different dataset D , specifically the training data used for learning the matching models.

As shown in Table V, when the input dataset D matches the set of query points, the calibration almost completely eliminates DP. However, when using the training data as D , DP is still reduced but not as effectively. This is because, although the training and test sets are drawn from similar distributions, they are not perfectly aligned. In fact, choosing an arbitrary dataset as D can even increase DP after calibration. Therefore, careful selection of dataset D is crucial.

Dataset	DeepMatch			DITTO		
	Before	D: Test	D: Train	Before	D: Test	D: Train
AMZ-GOO	8.90	0.09	1.13	5.73	0.09	1.67
DBLP-ACM	3.62	0.09	0.58	4.11	0.09	1.90
DBLP-GOO	6.15	0.07	1.71	5.8	0.07	2.68
ITU-AMZ	13.84	0.65	13.80	10.75	0.65	13.89

TABLE V: DP (%) before and after calibration using different input datasets D . “ D : Test” refers to using the same set of query points (i.e., test data) for calibration, while “ D : Train” uses the training data that was used to train the matcher.

VII. RELATED WORK

This section reviews fairness literature in record matching, ranking, and regression, highlighting connections to our work.

1) *Fairness in Record Matching*: Most existing work on fairness in record matching treats it as a binary classification task [6], [8], [11], evaluating fairness only through binary outcomes without addressing potential biases in matching scores. The most relevant prior work introduces a threshold-independent fairness metric based on AUC [7], but this can still be misleading in some cases [13]. Beyond defining such metrics, some studies propose bias reduction methods. For example, [44] train separate models per group, while [6] embed fairness constraints into matching process. Others, like [45], adjust tuple embeddings to preserve fairness alongside accuracy. Auditing tools have also been developed [46] to check fairness during training and testing. Finally, [8] provide a survey of fairness in matchers using standard fairness metrics.

2) *Fairness in Ranking*: Fair ranking aims to reduce bias when ordering items, typically by selecting k candidates from

n inputs. Methods are either score-based, assigning scores to rank items, or supervised, directly selecting the top- k without scoring [17]. While both fair ranking and score-based matching rely on scores, their goals differ: ranking emphasizes fair item positions, while matching focuses on producing unbiased scores without missing true matches. Our work treats matching as binary classification, where scores are intermediate values—similar to a k' -ranking with an unknown number of match pairs. Unlike ranking, which emphasizes proportional inclusion, we aim to align score distributions across groups to ensure fairness at all decision thresholds, as measured by metrics like demographic parity.

The work by [17] surveys fairness in score-based ranking, explaining how biased scores can cause unfair rankings. Similarly, [47] reviews fairness in supervised ranking, showing how bias in training data leads to unfair outcomes. Since supervised ranking does not use scores, post-processing adjustments are generally not applicable for it. In another work, [18] ensures protected groups are fairly represented in the top- k results through constrained optimization. Additionally, [19] focuses on fair rank aggregation by applying proportional representation while minimizing changes to the original rankings. Also, [48] introduces a policy method that balances individual and group fairness when learning ranking policies. Moreover, [49] provides a broad overview of fairness in ranking and recommendation systems, focusing on equitable visibility. Furthermore, [20] incorporates diversity constraints into ranking optimization to achieve balanced group representation. Finally, [21] formulates ranking as an optimization problem with fairness constraints, balancing fairness and relevance.

3) *Fairness in Regression:* Fairness-aware regression aims to predict continuous outcomes while reducing bias. This is closely related to fairness in record matching scores, as both involve assigning continuous values. In both cases, fairness focuses on aligning the distributions of these continuous outputs across demographic groups to prevent systematic differences. However, they have differences. Matching scores is used to decide if two records refer to the same entity, so fairness needs to ensure that scores are unbiased without harming the ability to detect true matches. In contrast, fair regression focuses on making accurate and unbiased predictions for individual outcomes. This makes fairness in matching more sensitive, as changing scores can hurt matching accuracy, making the trade-off between fairness and performance more challenging.

Many methods have been proposed to address bias in regression. For example, [16] transformed regression into a weighted classification problem. This approach adds fairness constraints into the optimization, balancing fairness with accuracy. Similarly, [15] introduces a method that uses Wasserstein barycenters to align the distribution of predictions across demographic groups, reducing bias while staying close to the original data. Additionally, [14] proposed a framework for fair regression by formulating fairness as a constrained optimization problem. This allows for different fairness goals, such as demographic parity and individual fairness, to be applied during training. In contrast, [50] focuses on fixing fairness issues after training by adjusting the regression outputs to ensure fair binary decisions at any threshold. Finally, in another study by [51], a minimax

optimization framework is presented to enforce demographic parity in regression while preserving accuracy.

VIII. CONCLUSION AND FUTURE WORK

This work focuses on biases in matching scores used in record matching, which cannot be detected or corrected using traditional fairness metrics designed for binary classification. Unlike binary labels, matching scores are used across various thresholds and directly influence downstream decisions such as ranking and human review. We show that existing state-of-the-art models can produce biased score distributions, even when they appear fair at specific thresholds. To address this, we introduce a threshold-agnostic measure of bias based on the statistical divergence between score distributions across demographic groups. Our evaluation demonstrates that this metric reveals biases overlooked by existing approaches and better captures fairness concerns in score-based systems.

To mitigate these biases, we propose two post-processing calibration algorithms that modify matching scores without altering the underlying models or requiring access to their training data. The first method, *Calib*, aligns score distributions across groups using the Wasserstein barycenter, effectively reducing DP bias. The second method, *C-Calib*, extends this idea to account for true labels, achieving fairness criteria such as EO and EOD. Both algorithms are model-agnostic and offer theoretical guarantees on fairness and risk. Empirical results across a range of datasets and models show that our methods significantly reduce bias while preserving predictive performance, offering a practical and principled approach for fairer record matching.

Future research could extend this work in several directions. Expanding calibration techniques to address additional fairness metrics beyond DP, EO, and EOD would make this approach more versatile. Exploring pre-processing and in-processing methods alongside post-processing calibration could provide a more complete understanding of the trade-offs between fairness, accuracy, and computational efficiency. Another valuable avenue involves examining biases throughout the entire record matching pipeline, including the blocking, matching, and resolution stages. An end-to-end analysis of how biases propagate and interact across these stages could lead to more comprehensive and fairness-aware entity resolution methods. Our calibration-based approach provides a strong foundation for improving fairness in record matching. Further exploration of extended bias metrics, pipeline-level bias analysis, and comparisons of different mitigation techniques will help build more fair and robust systems for record matching.

REFERENCES

- [1] J. Kasai, K. Qian, S. Gurajada, Y. Li, and L. Popa, “Low-resource deep entity resolution with transfer and active learning,” in *Proceedings of the 57th Annual Meeting of the Association for Computational Linguistics*. Association for Computational Linguistics, 2019, p. 5851.
- [2] V. V. Meduri, L. Popa, P. Sen, and M. Sarwat, “A comprehensive benchmark framework for active learning methods in entity matching,” in *Proceedings of the 2020 ACM SIGMOD international conference on management of data*, 2020, pp. 1133–1147.
- [3] S. Sarawagi and A. Bhadridipaty, “Interactive deduplication using active learning,” in *Proceedings of the Eighth ACM SIGKDD International Conference on Knowledge Discovery and Data Mining*, ser. KDD ’02. Association for Computing Machinery, 2002, p. 269–278.

[4] A. Elmagarmid, I. F. Ilyas, M. Ouzzani, J.-A. Quiané-Ruiz, N. Tang, and S. Yin, "Nadeef/er: generic and interactive entity resolution," in *Proceedings of the 2014 ACM SIGMOD International Conference on Management of Data*, ser. SIGMOD '14, 2014, p. 1071–1074.

[5] N. Shahbazi, J. Wang, Z. Miao, and N. Bhutani, "Fairness-aware data preparation for entity matching," in *2024 IEEE 40th International Conference on Data Engineering (ICDE)*, May 2024, pp. 3476–3489.

[6] V. Eftymiou, K. Stefanidis, E. Pitoura, and V. Christophides, "Fairer: Entity resolution with fairness constraints," in *Proceedings of the 30th ACM International Conference on Information & Knowledge Management*, ser. CIKM '21, 2021, p. 3004–3008.

[7] S. Nilforoushan, Q. Wu, and M. Milani, "Entity matching with auc-based fairness," in *2022 IEEE International Conference on Big Data (Big Data)*, Dec 2022, pp. 5068–5075.

[8] N. Shahbazi, N. Danevski, F. Nargesian, A. Asudeh, and D. Srivastava, "Through the fairness lens: Experimental analysis and evaluation of entity matching," *Proc. VLDB Endow.*, vol. 16, no. 11, p. 3279–3292, Jul. 2023.

[9] C. Fu, X. Han, J. He, and L. Sun, "Hierarchical matching network for heterogeneous entity resolution," in *Proceedings of the Twenty-Ninth International Joint Conference on Artificial Intelligence*, ser. IJCAI'20, 2021.

[10] N. Kallus and A. Zhou, "The fairness of risk scores beyond classification: Bipartite ranking and the xauc metric," in *Advances in Neural Information Processing Systems*, vol. 32, 2019.

[11] Z. Yang, Y. L. Ko, K. R. Varshney, and Y. Ying, "Minimax auc fairness: Efficient algorithm with provable convergence," *Proceedings of the AAAI Conference on Artificial Intelligence*, vol. 37, no. 10, pp. 11909–11917, Jun. 2023.

[12] R. Vogel, A. Bellet, and S. Clémenton, "Learning fair scoring functions: Bipartite ranking under roc-based fairness constraints," in *Proceedings of The 24th International Conference on Artificial Intelligence and Statistics*, ser. Proceedings of Machine Learning Research, vol. 130. PMLR, 13–15 Apr 2021, pp. 784–792.

[13] K. Kwegyir-Aggrey, M. Gerchick, M. Mohan, A. Horowitz, and S. Venkatasubramanian, "The misuse of auc: What high impact risk assessment gets wrong," in *Proceedings of the 2023 ACM Conference on Fairness, Accountability, and Transparency*, ser. FAccT '23, 2023, p. 1570–1583.

[14] J. Fitzsimons, A. Al Ali, M. Osborne, and S. Roberts, "A general framework for fair regression," *Entropy*, vol. 21, no. 8, 2019.

[15] E. Chzhen, C. Denis, M. Hebiri, L. Oneto, and M. Pontil, "Fair regression with wasserstein barycenters," in *Advances in Neural Information Processing Systems*, vol. 33, 2020, pp. 7321–7331.

[16] A. Agarwal, M. Dudik, and Z. S. Wu, "Fair regression: Quantitative definitions and reduction-based algorithms," in *Proceedings of the 36th International Conference on Machine Learning*, ser. Proceedings of ML Research, vol. 97. PMLR, 09–15 Jun 2019, pp. 120–129.

[17] M. Zehlike, K. Yang, and J. Stoyanovich, "Fairness in ranking, part i: Score-based ranking," *ACM Comput. Surv.*, vol. 55, no. 6, Dec. 2022.

[18] M. Zehlike, F. Bonchi, C. Castillo, S. Hajian, M. Megahed, and R. Baeza-Yates, "Fa*ir: A fair top-k ranking algorithm," in *Proceedings of the 2017 ACM on Conference on Information and Knowledge Management*, ser. CIKM '17, 2017, p. 1569–1578.

[19] D. Chakraborty, S. Das, A. Khan, and A. Subramanian, "Fair rank aggregation," in *Advances in Neural Information Processing Systems*, vol. 35. Curran Associates, Inc., 2022, pp. 23965–23978.

[20] K. Yang, V. Gkatzelis, and J. Stoyanovich, "Balanced ranking with diversity constraints," *Proceedings of the Twenty-Eighth International Joint Conference on Artificial Intelligence, IJCAI*, 2019.

[21] L. E. Celis, D. Straszak, and N. K. Vishnoi, "Ranking with Fairness Constraints," in *45th International Colloquium on Automata, Languages, and Programming (ICALP 2018)*, ser. Leibniz International Proceedings in Informatics (LIPIcs), vol. 107. Schloss Dagstuhl – Leibniz-Zentrum für Informatik, 2018, pp. 28:1–28:15.

[22] L. E. Celis, A. Mehrotra, and N. K. Vishnoi, "Interventions for ranking in the presence of implicit bias," in *Proceedings of the 2020 Conference on Fairness, Accountability, and Transparency*, ser. FAT* '20. Association for Computing Machinery, 2020, p. 369–380.

[23] A. Miroshnikov, K. Kotsopoulos, R. Franks, and A. Ravi Kannan, "Wasserstein-based fairness interpretability framework for machine learning models," *Machine Learning*, vol. 111, no. 9, pp. 3307–3357, 2022.

[24] C. Villani *et al.*, *Optimal transport: old and new*. Springer, 2008, vol. 338.

[25] M. Aguech and G. Carlier, "Barycenters in the wasserstein space," *SIAM Journal on Mathematical Analysis*, vol. 43, no. 2, pp. 904–924, 2011.

[26] M. Cuturi and A. Doucet, "Fast computation of wasserstein barycenters," in *Proceedings of the 31st International Conference on Machine Learning*, ser. Proceedings of Machine Learning Research, vol. 32, no. 2. PMLR, 22–24 Jun 2014, pp. 685–693.

[27] G. Peyré, M. Cuturi *et al.*, "Computational optimal transport: With applications to data science," *Foundations and Trends® in Machine Learning*, vol. 11, no. 5–6, pp. 355–607, 2019.

[28] P. A. Knight, "The sinkhorn–knopp algorithm: Convergence and applications," *SIAM Journal on Matrix Analysis and Applications*, vol. 30, no. 1, pp. 261–275, 2008.

[29] J. M. Chambers, *Graphical methods for data analysis*. Chapman and Hall/CRC, 2018.

[30] A. W. Van Der Vaart, *Asymptotic statistics*. Cambridge UP, 2000.

[31] L. Wasserman, *All of statistics: a concise course in statistical inference*. Springer Science & Business Media, 2013.

[32] S. Shalev-Shwartz and S. Ben-David, *Understanding machine learning: From theory to algorithms*. Cambridge UP, 2014.

[33] R. M. Dudley, *Uniform central limit theorems*. Cambridge university press, 2014, vol. 142.

[34] B. Neyshabur, R. Tomioka, and N. Srebro, "Norm-based capacity control in neural networks," in *Proceedings of The 28th Conference on Learning Theory*, ser. Proceedings of Machine Learning Research, vol. 40. PMLR, 03–06 Jul 2015, pp. 1376–1401.

[35] P. L. Bartlett, D. J. Foster, and M. J. Telgarsky, "Spectrally-normalized margin bounds for neural networks," in *Advances in Neural Information Processing Systems*, vol. 30. Curran Associates, Inc., 2017.

[36] C. Zhang, S. Bengio, M. Hardt, B. Recht, and O. Vinyals, "Understanding deep learning requires rethinking generalization," in *International Conference on Learning Representations*, 2017.

[37] D. Comaniciu and P. Meer, "Mean shift: a robust approach toward feature space analysis," *IEEE Transactions on Pattern Analysis and Machine Intelligence*, vol. 24, no. 5, pp. 603–619, 2002.

[38] anonymous, "Fair-em post-processing algorithm," <https://anonymous.4open.science/r/sigmod-FAIR-EM-post-process-C134>, 2025.

[39] S. Mudgal, H. Li, T. Rekatsinas, A. Doan, Y. Park, G. Krishnan, R. Deep, E. Arcaute, and V. Raghavendra, "Deep learning for entity matching: A design space exploration," in *Proceedings of the 2018 International Conference on Management of Data*, ser. SIGMOD '18, 2018, p. 19–34.

[40] M. H. Moslemi and M. Milani, "Threshold-independent fair matching through score calibration," in *Proceedings of the Conference on Governance, Understanding and Integration of Data for Effective and Responsible AI*, ser. GUIDE-AI '24, 2024, p. 40–44.

[41] D. Yao, Y. Gu, G. Cong, H. Jin, and X. Lv, "Entity resolution with hierarchical graph attention networks," in *Proceedings of the 2022 International Conference on Management of Data*, ser. SIGMOD '22. Association for Computing Machinery, 2022, p. 429–442.

[42] L. Yuliang, L. Jinfeng, S. Yoshihiko, D. AnHai, and T. Wang-Chiew, "Deep entity matching with pre-trained language models," *Proceedings of the VLDB Endowment*, vol. 14, no. 1, pp. 50–60, 09 2020.

[43] U. Brunner and K. Stockinger, "Entity matching with transformer architectures-a step forward in data integration," in *23rd International Conference on Extending Database Technology, Copenhagen, 30 March–2 April 2020*. OpenProceedings, 2020, pp. 463–473.

[44] C. Makri, A. Karakasidis, and E. Pitoura, "Towards a more accurate and fair svm-based record linkage," in *2022 IEEE International Conference on Big Data (Big Data)*, 2022, pp. 4691–4699.

[45] M. Ebraheem, S. Thirumuruganathan, S. Joty, M. Ouzzani, and N. Tang, "Distributed representations of tuples for entity resolution," *Proc. VLDB Endow.*, vol. 11, no. 11, p. 1454–1467, Jul. 2018.

[46] N. Shahbazi, M. Erfanian, A. Asudeh, F. Nargesian, and D. Srivastava, "Fairem360: A suite for responsible entity matching," *Proc. VLDB Endow.*, vol. 17, no. 12, p. 4417–4420, Aug. 2024.

[47] M. Zehlike, K. Yang, and J. Stoyanovich, "Fairness in ranking, part ii: Learning-to-rank and recommender systems," *ACM Comput. Surv.*, vol. 55, no. 6, Dec. 2022.

[48] A. Singh and T. Joachims, "Policy learning for fairness in ranking," in *Advances in Neural Information Processing Systems*, vol. 32, 2019.

[49] E. Pitoura, K. Stefanidis, and G. Koutrika, "Fairness in rankings and recommendations: an overview," *The VLDB Journal*, pp. 1–28, 2022.

[50] K. Kwegyir-Aggrey, J. Dai, A. F. Cooper, J. Dickerson, K. Hines, and S. Venkatasubramanian, "Repairing regressors for fair binary classification at any decision threshold," in *NeurIPS 2023 Workshop Optimal Transport and Machine Learning*, 2023.

[51] K. Fukuchi and J. Sakuma, "Demographic parity constrained minimax optimal regression under linear model," in *Advances in Neural Information Processing Systems*, vol. 36, 2023, pp. 8653–8689.